

Anisotropic Etching of Silicon in TMAH Solutions

Osamu Tabata*

Mechanical Engineering, Faculty of Science and Engineering, Ritsumeikan University
Noji-higashi, Kusatsu-shi, Shiga 525-8577, Japan

(Received May 15, 2000; accepted May 15, 2000)

Key words: TMAH, silicon, anisotropic etching

Anisotropic etching characteristics of tetramethyl ammonium hydroxide (TMAH) such as the dependences of the etching rates of (100), (110) and (111) crystal planes on temperature and concentration, the selectivity to SiO_2 and Si_3N_4 , electrochemical etching characteristics, aluminum etching rate dependences on pH and conductivity and the effect of potassium ion addition are reviewed. Furthermore, the preliminary results obtained by the approach using a molecular orbital program are briefly introduced.

1. Introduction

Anisotropic etching of silicon is a key technology for fabricating various three-dimensional structures for micro-electromechanical systems (MEMS). Although deep reactive ion etching (deep RIE) has become popular for realizing high-aspect-ratio silicon microstructures, the advantages of silicon anisotropic etching technology such as low process cost, better surface smoothness and less environmental pollution makes it a useful technology.

Any solution with a pH value larger than 12 can be used as an anisotropic etching solution. However, the anisotropic etching solution for silicon micromachining is required to have good anisotropic etching characteristics such as a high etching rate of silicon, high etching rate dependences on crystallographic orientations, a smooth etched surface, a low etching rate of mask material, compatibility with the CMOS process, low toxicity and easy handling. From these viewpoints, many etchants including inorganic aqueous solutions of KOH,⁽¹⁾ NaOH,⁽²⁾ CsOH,⁽³⁾ NH_4OH ,⁽⁴⁾ hydrazine⁽⁵⁾ as well as organic aqueous solutions

*Corresponding author, e-mail address: tabata@se.ritsumei.ac.jp

containing ethylenediamine (EDP),⁽⁶⁾ choline⁽⁷⁾ and tetramethyl ammonium hydroxide (TMAH, $(\text{CH}_3)_4\text{NOH}$)^(8,9) have been proposed. Representative etchants and their characteristics are summarized in Table 1. Among these etchants, TMAH and KOH are the most commonly used etchant for MEMS fabrication.

TMAH has become popular because of its high compatibility with the CMOS process, easy handling and low toxicity. Furthermore, semiconductor-grade solutions can be easily obtained because TMAH has been utilized in the LSI process as the developing solution of a positive photoresist. TMAH is a kind of quaternary ammoniumhydroxide (QAH) solution that was proposed by Asano⁽⁷⁾ in 1976 as an etching and cleaning solution for silicon and silicon-dioxide surfaces. Detailed characteristics of QAH as a silicon anisotropic etchant were not reported until 1990. Characteristics of tetraethyl ammonium hydroxide (TEAH), which is a class of QAH, were reported by our group⁽⁸⁾ in 1990, and those of TMAH were reported by us and by Schnakenberg *et al.* in 1991.^(9,10)

In this study, various anisotropic etching characteristics such as the dependences of the etching rates of (100), (110) and (111) crystal planes on temperature and concentration, selectivity to SiO_2 and Si_3N_4 , electrochemical etching characteristics, aluminum etching rate dependences on pH and conductivity and the effect of potassium ion addition to TMAH were reviewed. Furthermore, preliminary results obtained by the approach using a molecular orbital program are briefly introduced as a recent research approach.

2. Etching Characteristics of TMAH

2.1 Etching rate of (100), (110) and (111)

Three-inch (100)-oriented n-type silicon wafers with resistivities of 30–50 $\Omega\text{-cm}$ were used in the experiments. Either thermally oxidized SiO_2 or low pressure chemical vapor deposition (LPCVD)-deposited Si_3N_4 was used for an etching mask. The etching test patterns were 2.5-mm-square windows. Etching was carried out with no stirring in a glass vessel thermostated with a temperature bath. A reflux condenser was used to avoid changing the concentration during the etching. Each sample was held horizontally. Etching solutions were prepared by condensation or dilution of commercially available

Table 1

Comparison of characteristics of the representative silicon anisotropic etchants.

Solution	(100)/(111) etching rate ratio	(100)/ SiO_2 etching rate ratio	CMOS process compatibility	Handling
KOH	HIGH	LOW	LOW	EASY
NaOH	HIGH	LOW	LOW	EASY
EDP	LOW	HIGH	MIDDLE	HARD
N_2H_4	LOW	HIGH	MIDDLE	TOXIC
NH_4OH	LOW	HIGH	HIGH	HARD
TMAH	LOW	HIGH	HIGH	EASY

TMAH with a concentration of 22 wt% (TCL-22, KANTO CHEMICAL Corp.). The etching depth was mechanically measured using an electronic micrometer. The etching rates of the (111) plane were calculated from the optically measured side etching distance, considering the cross-angle of (111) and (100) planes.

The dependences of the (100) etching rates on concentration and temperature are shown in Fig. 1. The etching rates decrease with increasing concentration. At 5 wt%, the etched surface was sometimes covered by pyramidal-shaped hillocks and the etching rate became very low. Therefore, the etching rates of (100) planes exhibit a maximum at a concentration of approximately 5 wt%. As the concentration increases, the smoothness of the etched (100) surface changes drastically. Figure 2 shows secondary electron microscope (SEM) micrographs of the (100) surface etched for 90 min at a temperature of 70°C and concentrations from 5 to 40 wt%. At 5 wt%, the surface was covered by pyramidal hillocks in high densities. With an increase in concentration from 5 to 15 wt%, the density of the hillocks decreased and smaller hillocks were obtained. The hillocks were bounded by (111) crystal planes. Above 22 wt%, a very smooth surface was observed. The measured roughness for the 22 wt% solution was within 100 nm.

The etching rate of (110) is about 1.4 times larger than that of (100). The dependences of the (110) etching rates on concentration and temperature are similar to those of (100). Etched surface morphologies of the (110) plane were different from (100). Triangular columnar structures directed to $\langle 110 \rangle$ orientation were observed. The height of the columnar structures decreases with increasing concentration and a smooth surface is obtained above 30 wt%.

Figure 3 shows the dependences of the (111) etching rates on concentration and temperature, which show a tendency similar to those of (100) and (110). The etching rate of (111) is about 0.02–0.05 times smaller than that of (100). The (100)/(111) etching rate ratio was calculated to be 35 at 5 wt% and 90°C. This value decreases with decreasing

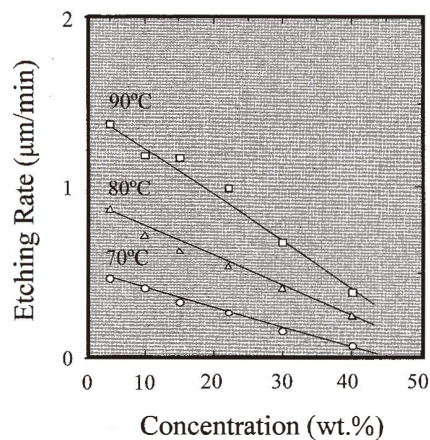


Fig. 1. Dependences of (100) etching rate on temperature and concentration.

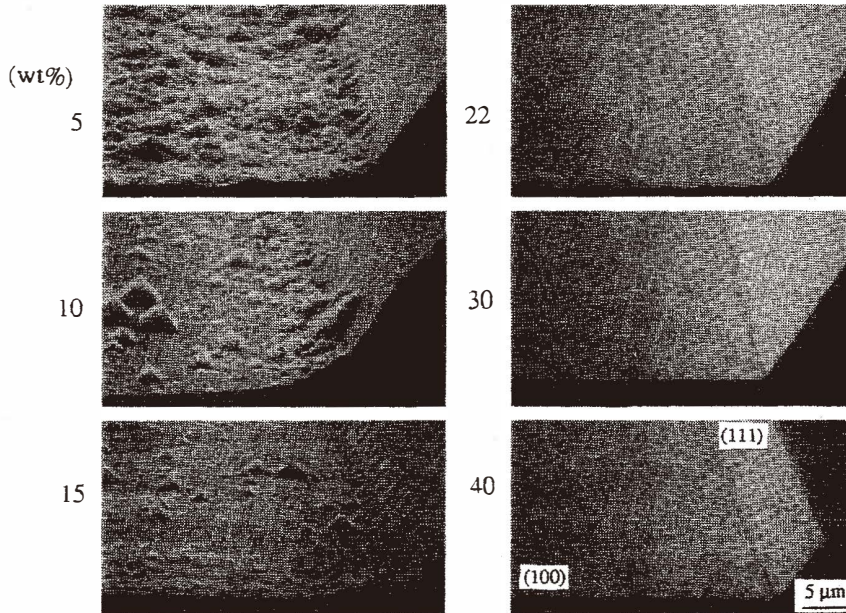


Fig. 2. SEM micrographs of the (100) surface etched for 90 min at a temperature of 70°C and concentrations between 5 and 40 wt%.

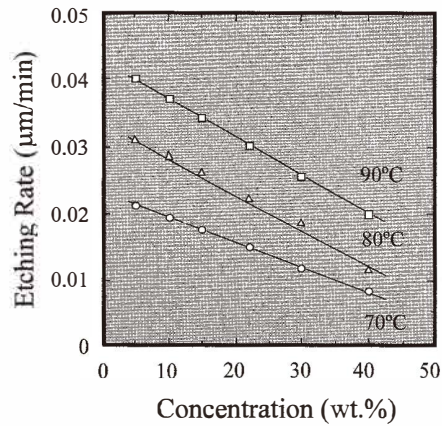


Fig. 3. Dependences of (111) etching rate on temperature and concentration.

temperature and increasing concentration. The etching rate ratio of 10 was observed at 40 wt% and 70°C. Since it is almost one order of magnitude lower than that of KOH, TMAH is not suitable if smaller side etching is required.

The activation energies were calculated for (100), (110) and (111) planes, and were 0.5–0.7 eV, 0.4 eV and 0.4 eV, respectively. The activation energy of (100) increases with increasing concentration. This indicates that the etching rate ratio of (100)/(111) increases with increasing temperature and concentration.

2.2 Etching rate of SiO_2 and Si_3N_4

The etching rates of SiO_2 and Si_3N_4 were determined by ellipsometric measurements. The etching rate of SiO_2 is almost four orders of magnitude lower than that of (100). The activation energy was calculated to be approximately 0.9 eV, which is larger than those for (100), (110) and (111) planes. Therefore, the selectivity of SiO_2 to (100), (110) and (111) planes increases with decreasing temperature.

In comparison with KOH, TMAH shows an etching rate two orders of magnitude lower than that of SiO_2 . This low etching rate of SiO_2 is one of the features of TMAH. It was demonstrated that the potassium ion concentration in solution strongly affects the etching rate of SiO_2 . By adding 0.5 g/L of potassium ions to TMAH, the etching rate of SiO_2 increased by one order of magnitude.⁽¹¹⁾

LPCVD-deposited Si_3N_4 exhibited almost no etching rate within the accuracy of the measurement. Thus, it appeared that SiO_2 and Si_3N_4 could be used as excellent etching masks for TMAH.

2.3 Electrochemical etching of (100)

The experimental setup for electrochemical etching is schematically shown in Fig. 4. A potentiostat and a wave generator were used to control the potential of the silicon sample with respect to an Ag/Ag-Cl reference electrode (RE), while a platinum electrode acted as a counterelectrode (CE). The Ag/Ag-Cl reference electrode was selected since it can be used as a stable reference electrode up to 90°C. Most of the experiments were carried out at 80°C in the 22 wt% TMAH solution with no stirring. The samples used were (100)-oriented n-type and p-type silicon wafers with resistivities from 0.01 to 10 $\Omega\text{-cm}$, corresponding to impurity concentrations of approximately 5×10^{14} to $1 \times 10^{19}/\text{cm}^3$. LPCVD-deposited Si_3N_4 was used for etching masks. The etching test patterns of 2.5-mm-square windows were formed on the front side of the wafer. Electrical contact areas were fabricated by means of ion implantation and the deposition of an aluminum layer on the back surface of the wafer. Samples of $1 \times 3 \text{ cm}^2$ were cut out from the wafers and submerged vertically in the etching solution. Except for the window pattern, the sample was covered with wax. To generate current-potential curves, the applied potential was swept from negative to positive with a sweep rate of 200 mV/min.

The measured open-circuit potential (OCP) and passivation potential (PP) were -1.66 V and -1.00 V for a p-type 10 $\Omega\text{-cm}$ sample, and -1.72 V and -1.11 V for an n-type 10 $\Omega\text{-cm}$ sample, respectively. The dependences of these voltages on the resistivity were very small. The PP slightly increased with decreasing concentration. On the other hand, the

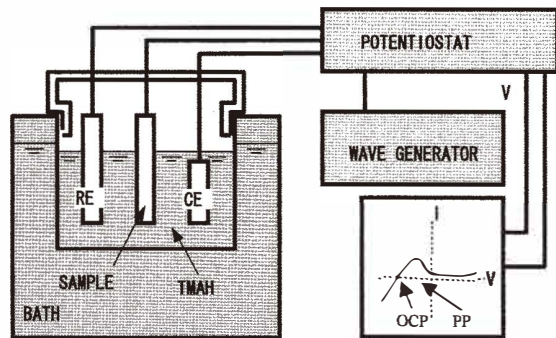


Fig. 4. Setup for electrochemical etching.

OCP was not affected by concentration. These potentials were very close to those obtained for KOH solutions.

The etching rates for p-type and n-type (100) were reduced to nearly zero by applying a potential above PP to the sample. The reduction of the etching rate of n-type silicon was less drastic than that of p-type silicon.

2.4 Dependence of aluminum etching rate on the amount of dissolved silicon

Several groups have demonstrated that fabricating MEMS devices with integrated CMOS circuits becomes possible by adding a sensor process to the standard CMOS process.^(12,13) Anisotropic etching is required in the added sensor process. This so-called post-CMOS processing approach is very attractive from the viewpoint of pushing these devices to mass production. The etching characteristic required for the anisotropic etching solution used in the post-CMOS processing approach is selectivity to aluminum. This is because aluminum is used for metallization in the standard CMOS and is exposed at the bonding pads of the circuits. The etching solutions used most commonly for the post-CMOS process are hydrazine and EDP; however, hydrazine is highly toxic and EDP requires handling with caution. A promising candidate is silicon dissolved in TMAH.

The measured dependences of the aluminum etching rate on the amount of dissolved silicon in TMAH with 10 wt% and 22 wt% at 80°C are shown in Fig. 5. By increasing the amount of dissolved silicon, the etching rate of aluminum decreased slightly first and then decreased abruptly. In order to lower the etching rate to less than 0.01 $\mu\text{m}/\text{min}$, it is required to dissolve the silicon to a concentration of 1.25 mol/L and 3.2 mol/L for 10 wt% TMAH and 22 wt% TMAH solution, respectively.

It is thought that the aluminum surface is protected from the etchant by the aluminosilicate passivation layer formed during the etching.⁽⁸⁾ The amount of silicon required to form this passivation layer is not great. However, the pH must be low to form the passivation layer. It is well known that the hydroxide ion is consumed by the etching reaction. Therefore, the pH of the etching solution decreases with the increasing amount of dissolved silicon. Namely, the addition of silicon in TMAH lowers the pH.

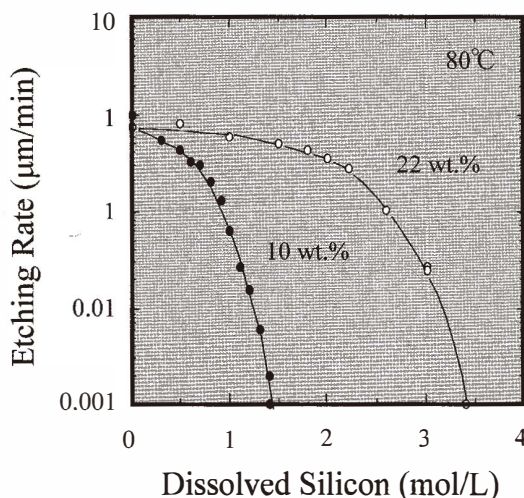


Fig. 5. Dependence of aluminum etching rate on the amount of dissolved silicon.

If low pH plays an important role in forming the alumino-silicate passivation layer, it should be possible to passivate the aluminum layer by lowering the pH of TMAH by adding acid such as $(\text{NH}_4)_2\text{CO}_3$ and $(\text{NH}_4)\text{HPO}_4$.⁽¹⁴⁾ This insight was confirmed through experiments.

The dependence of the aluminum etching rate on the amount of added $(\text{NH}_4)\text{HPO}_4$ for 10 and 22 wt% TMAH containing dissolved silicon of 0.66 mol/l was measured. As observed in silicon dissolution experiments, the aluminum etching rate decreased slightly at first and then decreased abruptly with the increasing amount of added acid. The dependences of the aluminum etching rate on the pH values for TMAH with acid added were determined. For obtaining an aluminum etching rate of 0.01 $\mu\text{m}/\text{min}$, it appears that the required pH values are 11.5 for 10 wt% TMAH with $(\text{NH}_4)_2\text{CO}_3$ and $(\text{NH}_4)\text{HPO}_4$ added. The required pH values were 12 for 22 wt% TMAH with $(\text{NH}_4)_2\text{CO}_3$ or $(\text{NH}_4)\text{HPO}_4$ added. These pH values are identical to those obtained for silicon dissolution. These results prove that the decrease in the aluminum etching rate to 0.01 $\mu\text{m}/\text{min}$ can also be achieved by adding acid to control the pH value to 11.5 for 10 wt% TMAH and 12 for 22 wt% TMAH.

However, if the pH of the TMAH decreases too much by dissolving an excess amount of silicon or acid, the etching rate of silicon decreases and the etched surface becomes rough. Note that the etching rate of silicon decreases and the etched surface become rough by decreasing the concentration to less than 5 wt%, as shown in Figs. 1 and 2. Both of these phenomena are caused by lowering the pH of the TMAH. To realize a low aluminum etching rate with a certain silicon etching rate and a smooth etched surface, the pH should be controlled to a certain value.

2.5 pH and σ of TMAH

Since the hydroxide ion plays an important role in anisotropic etching, pH can be used as an index of the solution. However, less attention has been paid to the conductivity (σ) of the solution.^(14,15)

The σ of a solution is defined by the charge, mobility and concentration of all ionic species in the solution. Major ions in the etching solution are hydrated cations and hydroxide ions. Because the mobility of hydrated cations is thought to be smaller than that of hydroxide ions, the measured value of σ is thought to reflect the concentration and mobility of hydroxide ions. Because the concentration of the hydroxide ion can be determined from pH values, differences in hydroxide ion mobility can be monitored by measuring both pH and σ .

TMAH at a concentration of 22 wt% was used, and solutions with lower concentrations were prepared by dilution with deionized water. Experiments on dissolved silicon were carried out with silicon dissolved at 0.3 to 4.0 mol/l in TMAH. The pH and σ of the TMAH were measured using a pH meter (HORIBA Corp.) and a conductivity meter (YOKOGAWA Corp.). Etching was carried out with no stirring in a glass vessel thermostated in a temperature bath at 80°C.

Figure 6 shows the dependence of the Si(100) etching rate on pH for diluted TMAH and silicon dissolved in TMAH. The etching rates decreased with the increasing pH value. These dependences coincide with the fact that the etching rate decreases with increasing TMAH concentration above 5 wt%. However, the etching rates for diluted TMAH and TMAH with dissolved silicon did not coincide.

To clarify the reason for this difference in the Si(100) etching rate, the relationships between pH and σ for silicon dissolved in 22 wt% TMAH and diluted 22 wt% TMAH were investigated. The results are shown in Fig. 7. In a certain range of pH, values of σ for

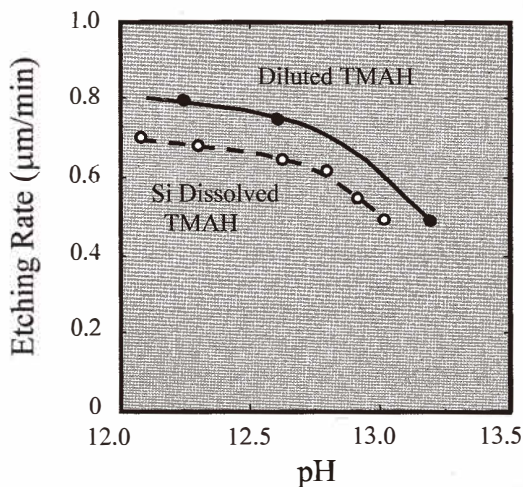


Fig. 6. Dependence of the Si(100) etching rate on pH for diluted TMAH and Si dissolved in TMAH.

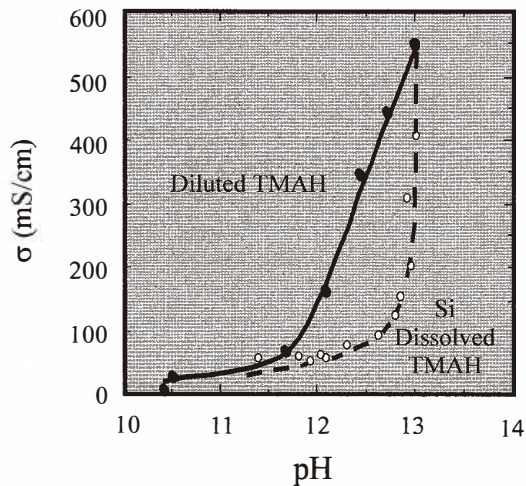


Fig. 7. Relationships between pH and σ for silicon dissolved in 22 wt% TMAH and diluted 22 wt% TMAH.

TMAH with dissolved silicon were lower than those of diluted TMAH at the same pH. This suggests that the mobility of the hydroxide ion in the TMAH with dissolved silicon is lower than that in the diluted TMAH. This difference in mobility is thought to be caused by the etching products in the solution. This difference in mobility of the hydroxide ion is thought to affect the Si(100) etching rate. The experimental results strongly suggest that products of etching affect the etching reaction.

2.6 Effect of potassium ion addition

Thus far, little attention has been paid to the role of cations on the anisotropic etching characteristics. However, in order to reveal the anisotropic etching mechanism, the role of cations is important. As previously mentioned, it was confirmed that potassium ions caused a significant change in the SiO_2 etching rate of TMAH. The potassium ion addition to TMAH also strongly affects the etching rate distribution of all crystallographic orientations.⁽¹⁶⁾

A solid hemispherical specimen of single-crystal silicon was used to measure the etching rate distribution of all crystallographic orientations precisely. The radius of the hemisphere was 22 mm, and its sphericity was less than $10 \mu\text{m}$.⁽¹⁷⁾ Three different etchants, KOH, TMAH, and TMAH with added K_2CO_3 , were used as etchants. The concentration of KOH solution is 35 wt% with a temperature of 70°C . The concentration of TMAH solution is 20 wt% with a temperature of 80°C . The amount of added K_2CO_3 is 0.5 g/L. This amount of added K_2CO_3 was chosen since it has been confirmed through previous experiments that the effect of potassium ion addition is most evident at this concentration.

Figure 8 shows the etching rate distribution along the line on the stereographic diagram from the (111) plane to the (011) and from the (011) to the (001) plane. From these experiments, it is clear that the etching rate in the $\langle 011 \rangle$ direction decreases dramatically with the addition of potassium ions. The etching rate of the $\langle 011 \rangle$ direction became nearly equal to that of the $\langle 001 \rangle$ direction and the $\langle 011 \rangle / \langle 001 \rangle$ etching rate ratio decreased from 1.57 to 1.03. The etching rate of the $\langle 111 \rangle$ direction increased slightly with the addition of potassium ions. It is very interesting that the characteristics of TMAH with potassium ions are not similar to those of KOH. The mechanism of the effect of added potassium ions remains to be clarified.

3. Approach Using Molecular Orbital Program

The etching characteristics do not depend only on concentration and temperature but also on parameters such as stirring conditions, additives and degradation of the etchant. It is not practical to measure the etching rate for all crystallographic orientations under all such conditions. If we can identify a few parameters that dominate the etching rate for all crystallographic orientations, it will be possible to reconstruct etching rates for all crystallographic orientations from these parameters. For the extraction of the dominant parameters, a simulation based on the physics of atomic-scale phenomena is promising⁽¹⁸⁻²¹⁾. In this approach, only a few parameters are required to predict the etching rate for all crystallographic orientations.

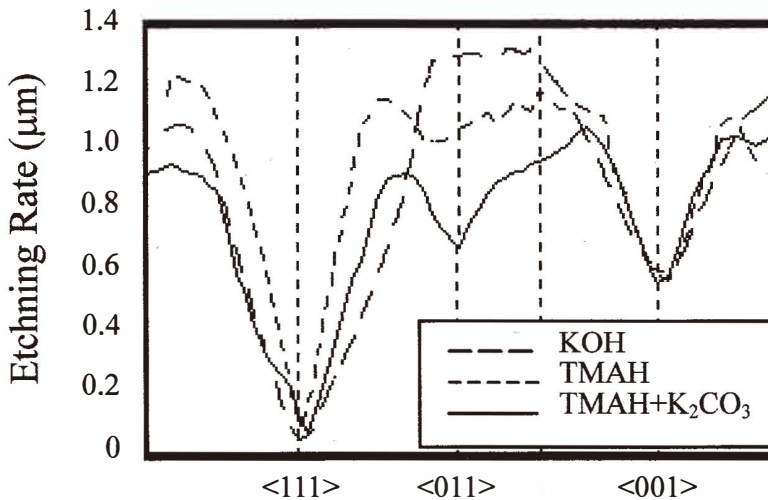


Fig. 8. Etching rate distribution along the line from the (111) plane to (011) and from (011) to the (001) plane.

The key point is the selection of parameters. It makes sense to select parameters from the viewpoint of crystallographic growth science. By analogy to the crystallographic growth mechanism, etching rates are thought to be limited by (1) etching kinetics at the crystal surface and (2) diffusion in the solution. Concerning etching kinetics, the importance of energy to add or remove atoms from the surface is obvious. Recent progress in computer technology makes it possible to approach this problem by means of a molecular orbital simulation.

As the first step, the commercially available molecular orbital simulation program MOPAC was used to calculate the energy difference before and after the removal of atoms from the (100), (110) and (111) planes. Figure 9 shows an example of the models utilized to calculate the energy change before and after atom removal. The silicon crystal is composed of about 200 atoms and it is assumed that the surface is covered by absorbed hydroxide ions. Energy changes before and after atom removal were calculated to be -24.02 , 261.70 and -82.52 (kcal/mol) for (100), (110) and (111), respectively. Here, the negative sign means that additional energy is required for this reaction. Therefore, (110) is the fastest etching plane and (111) is the slowest.

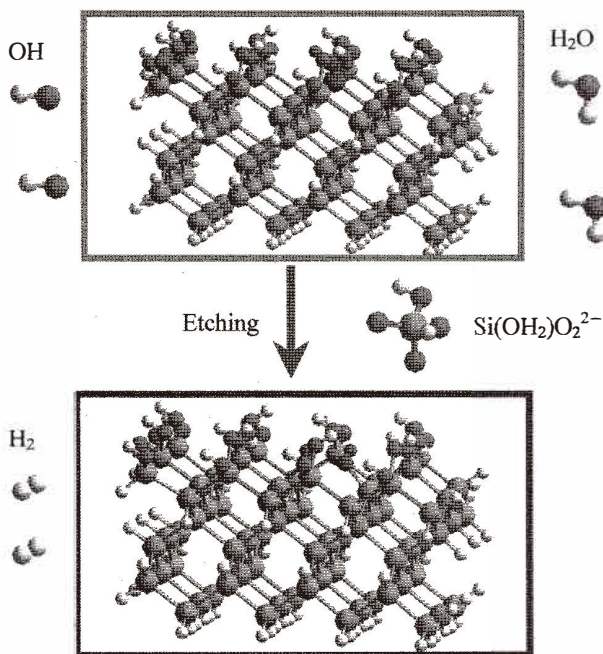


Fig. 9. Models utilized to calculate the energy change by the molecular orbital simulation program MOPAC.

In order to take into account practical etching parameters such as hydroxide ion concentration, various cations and their concentrations, etching products and additives, further study is required. However, molecular orbital simulation is undoubtedly a promising and powerful approach in this field.

4. Conclusions

A series of experiments have been carried out to reveal the basic etching characteristics and effect of additives to TMAH on etching. The etching characteristics of TMAH are summarized in Table 2 through comparison with KOH. Due to its superior characteristics, the importance of TMAH is expected to increase. The final goals of this research are to understand the principle which dominates etching characteristics and to make it possible to control these etching characteristics to realize more complicated three-dimensional silicon microstructures.

Table 2
Comparison of TMAH and KOH characteristics.

	TMAH 90°C, 22 wt%	KOH 90°C, 20 wt%
(100) etching rate ($\mu\text{m}/\text{min}$)	1.0	2.5
(110) etching rate ($\mu\text{m}/\text{min}$)	1.4	3.8
Surface roughness (nm)	<100	<100
(111)/(100) etching rate ratio	0.033	2.5×10^{-3}
SiO ₂ etching rate (nm/min)	0.23	9.6
Si ₃ N ₄ etching rate (nm/min)	<0.01	<0.01

References

- 1 H. R. Huff and R. R. Burgess: *Semiconductor Silicon*, (Electrochemical Society Softbound Proceedings Series, Princeton, NJ USA, 1973) 339.
- 2 I. J. Pugacz-Muraszkiewicz: *IBM J. Res. Develop.* **16** (1972) 523.
- 3 L. D. Clark Jr, J. L. Lund and D. J. Edell: *Technical Digest, IEEE Solid-State Sensor and Actuator Workshop, Hilton Head Island, S.C., USA* **5** (1988)
- 4 U. Schnakenberg, W. Benecke and B. Lochel: *Sensors and Actuators A21–A23* (1989) 1031.
- 5 M. J. Declercq, L. Gerzberg and J. D. Meindl: *J. Electrochem. Soc.* **122** (1975) 545.
- 6 A. Reisman, M. Berkenblit, S. A. Chan, F. B. Kaufman and D. C. Green: *J. Electrochem. Soc.* **126** (1979) 1406.
- 7 M. Asano, T. Cho and H. Muraoka: *Electrochem. Soc. Ext. Abstr.* **354** (1976) 911.
- 8 O. Tabata, R. Asahi and S. Sugiyama: *Technical Digest of the 9th Sensor Symposium* **15** (1990)

- 9 O. Tabata, R. Asahi, H. Funabashi and S. Sugiyama: *Tec. Dig. of Int. Conf. on Solid-State Sensors and Actuators* **811** (1991)
- 10 U. Schnakenberg, W. Benecke and P. Lange: *Proc. of 6th Int. Conf. Solid-State Sensors and Actuators* **24** (1991)
- 11 O. Tabata: *Trans. IEE of Japan*. 118-E **5** (1998) 278.
- 12 N. Fujitsuka, J. Sakata, Y. Miyachi, K. Mizuno, K. Ohtsuka, Y. Taga and O. Tabata: *Sensors and Actuators* **A66** (1998) 237.
- 13 M. Gaitan, J. Kinard and D. X. Huang: *The 7th International Conference on Solid-State Sensors and Actuators* (1993) p.1012.
- 14 O. Tabata: *Sensors and Actuators A* **53** (1996) 289.
- 15 O. Tabata: *Sensors and Materials* **10** (1998) 425.
- 16 O. Tabata, M. Yashima, T. Yoshioka and K. Sato: *The 10th Int. Conf. on Solid-State Sensors and Actuators* (1999) p.542.
- 17 K. Sato, M. Shikida, T. Yamashiro, K. Asaumi, Y. Irie and M. Yamamoto: *The 11th Int. Conf. On Micro Electro Mechanical Systems* (1998) 556.
- 18 H. Camon, M. Djafari-Rouhani, D. Esteve, A. M. Gue and Z. Moktadir: *Microsystem Technologies* **1** (1995) 163.
- 19 P. J. Hesketh, C. Ju and S. Gowda; *Journal of Electrochemical Society* **140** (1993) 1080.
- 20 C. H. Sequin: *International Conference on Solid State Sensors and Actuators* (1991) p.801.
- 21 J. van Suchtelen, K. Sato, E. van Veenendaal, A. J. Nijdam, J. G. E. Gardeniers, W. J. P. van Enkevort and M. Elwenspoek: *Proceedings of the IEEE Micro Electro Mechanical Systems* (1999) p.332.